Methacrylated BSA and Tannic Acid Composite Materials for 3D Printing Tough and Mechanically Functional Parts

*Patrick T. Smith, Gokce Altin[†], S. Cem Millik, Benjaporn Narupai, Cameron Sietz, James O. Park[‖], and Alshakim Nelson**

Department of Chemistry, University of Washington, Seattle, Washington 98195, USA

Keywords: protein-based materials, tannic acid, tough hydrogels, bioplastics, bovine serum albumin, 3D printing

Abstract

Nature utilizes proteins as building blocks to create 3D structural components (like spiderwebs and tissue) that are recycled within a closed loop. Furthermore, it is difficult to replicate the mechanical properties of these 3D architectures within synthetic systems. In the absence of biological machinery, protein-based materials can be difficult to process and can have a limited range of mechanical properties. Herein, we present an additive manufacturing workflow to

fabricate tough, protein-based composite hydrogels and bioplastics with a range of mechanical properties. Briefly, methacrylated bovine serum albumin-based aqueous resins were 3D printed using a commercial vat photopolymerization system. The printed structures were then treated with tannic acid (TA) to introduce additional non-covalent interactions and form tough hydrogels. The hydrogel material could be sutured and withstand mechanical load even after immersion in water for 24 h. Additionally, a denaturing thermal cure could be used to virtually eliminate rehydration of the material and form a bioplastic. To highlight the functionality of this material, a bioplastic screw was 3D printed and driven into wood without damage to the screw. Moreover, the 3D printed constructs enzymatically degraded up to 85% after 30 days in pepsin solution. Thus, these protein-based 3D printed constructs show great potential for biomedical devices that degrade *in situ.*

1. Introduction

The growing use of plastics and rapid accumulation of plastic waste calls for the development of alternative materials that are promptly degradable and environmentally benign.[1–3] Proteins represent a class of biopolymers with remarkable structural and functional diversity. Utilizing proteins for commercial materials applications can reduce our reliance on petroleum-based materials, as protein feedstocks can be obtained in high volumes from microbial, plant, and animal sources.[4–6] Proteins also represent a platform for creating a circular economy for recycling.[7] Silk fibroin, collagen, gelatin, and bovine serum albumin (BSA) are examples of proteins and protein derivatives that have thus far been investigated for materials applications that range from commodity materials to specialized biomedical materials. Protein-based materials can generally be processed via solvent casting, melt extrusion, and injection molding,[8] however, their application is limited by poor processability into 3D form factors coupled with poor mechanical performance.[9]

Vat photopolymerization[10,11] 3D printing techniques such as stereolithographic apparatus (SLA) 3D printing, digital light processing (DLP), continuous liquid interface production (CLIP),[12] and high-area rapid printing (HARP)[13] have emerged as promising techniques that offer high quality parts at increasingly fast production rates.[14] The list of 3D printable elastomers, plastics, and composites reported in the literature continues to grow; however, most of these materials are not biodegradable, and only a few are based on biopolymers.[15–19] The design of photocurable resins for vat photopolymerization requires photo-crosslinkable molecules with low intrinsic viscosities and fast photocuring rates. In general, a low resin viscosity (0.25 Pa·s to 10 Pa·s)[10,20,21] is necessary to facilitate resin reflow and minimize the undesirable stresses exerted on the printed object during the printing process.[22–24] The polymer concentration should be maximized in a resin formulation. Yet, increasing the polymer concentration in the resin increases viscosity, as does increasing the molecular weights of the polymeric components, as predicted by Mark-Houwink equation.[25] An alternative design strategy is to employ synthetic polymers with cyclic, branched, or dendritic architectures, or cross-linked unimolecular particles. These architectures are characterized by low intrinsic viscosities relative to that of a linear polymer counterpart.[26–29] Interestingly, the majority of photocurable protein derivatives that have been reported are based on structural proteins (e.g., gelatin and silk fibroin),[18,19] which form fibrous higher-order assemblies. Anisotropic structures or macromolecules that undergo significant entanglement is undesirable in vat photopolymerization processes, as this substantially increases the resin viscosity, which can limit processability.

BSA is a globular protein that is well suited for vat photopolymerization 3D printing.[30] At around neutral pH, BSA is highly aqueous soluble (up to 50 wt %) largely due to its high surface charge. Additionally, BSA has a low intrinsic viscosity, which is related to its compact nanoparticle-like

structure. Together, the high solubility and low intrinsic viscosity of BSA facilitate high BSA loading into resins as well as facile processing of BSA-based resins. Methacrylated BSA (MABSA) was synthesized by functionalizing available surface lysines of BSA.[30] Unlike gelatin methacrylate (GelMA),[31,32] MABSA does not naturally form physical hydrogels at moderate concentrations (2–40 wt %) in water. We reported this photo-crosslinkable derivative of BSA for vat photopolymerization 3D printing using a commercially available Form 2 SLA 3D printer.[30] While mechanically stiff (6 MPa) hydrogels were reported,[30] the applicability of these materials for a broader array of load-bearing applications was limited by their swelling in water, which reduced their mechanical strength.[33,34] Additionally, poly(ethylene glycol) diacrylate (PEGDA) was necessary for network formation but also precluded complete enzymatic degradation of the material (Table S1).

Tannic acid (TA) is a plant-sourced polyphenol that has been shown to enhance the mechanical properties of synthetic and biopolymer hydrogels.[33,35–43] TA can introduce secondary crosslinks within polymeric networks through hydrogen bonding and hydrophobic interactions[44–46] to enhance the elastic modulus, strength, and toughness of a hydrogel. Additionally, the noncovalent interactions with TA can reduce the extent of swelling of a polymer network and provide sacrificial bonds as an energy dissipation mechanism that improves toughness.

Herein, we present a process for fabricating biodegradable 3D constructs from a MABSA-TA composite material, which can be used either as a tough hydrogel or dehydrated bioplastic.[47] We developed resin formulations for SLA 3D printing that comprised MABSA and water-soluble acrylate monomers. The mechanical properties of these as-printed hydrogel constructs could be enhanced with the incorporation of TA into the crosslinked MABSA network. MABSA-TA composite hydrogels had greater toughnesses than the as-printed counterparts; this was afforded

by the incorporation of the secondary noncovalent crosslinks introduced by TA. In a subsequent step, MABSA-TA composites were thermally cured at 120 °C to unfold α-helical regions and concomitantly form β-sheet structures,[48,49] thereby enhancing mechanical properties. We refer to thermally denatured MABSA-TA (dMABSA-TA) composites as bioplastics. The presence of TA in these bioplastics enhanced mechanical properties and prevented rehydration of these materials when immersed in water. The improvements in ultimate strength, elastic modulus, and toughness for these protein-based materials enabled 3D printed constructs that were mechanically functional, such as screws and suturable devices. To the best of our knowledge, this is the first reported demonstration of a biodegradable and 3D printable hydrogel that can hold a suture after immersion in water for at least 24 h.

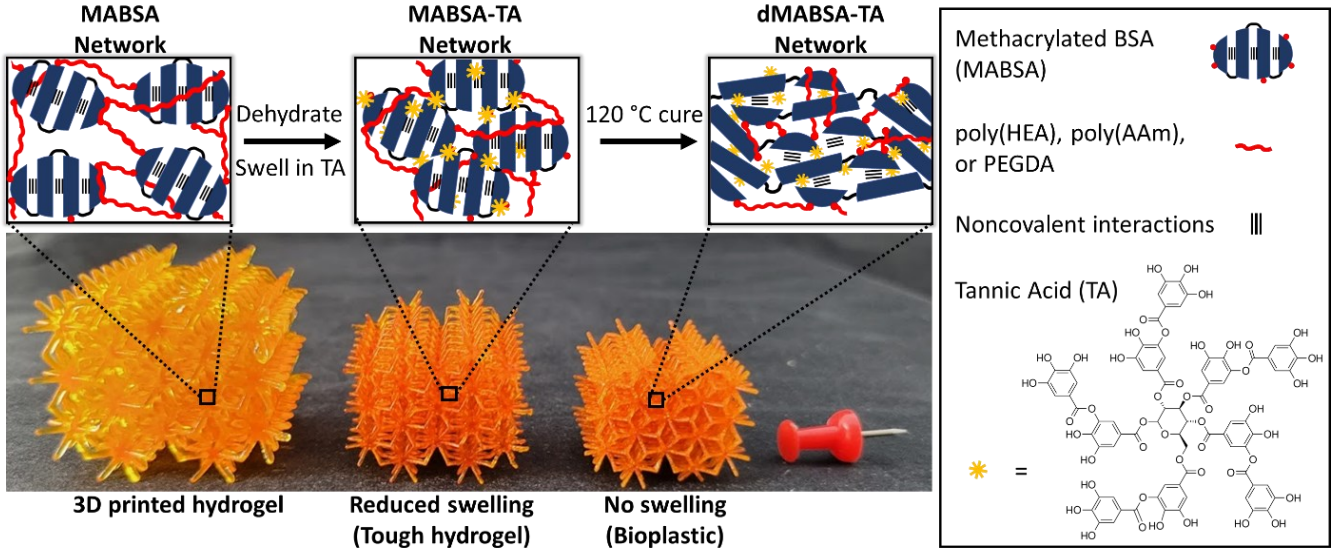

Figure 1. SLA 3D printed MABSA lattice structures. Swelling in water of the as-printed hydrogel constructs was reduced by TA treatment. This TA treatment also increased toughness of the (resultant MABSA-TA) hydrogel. An additional 120 °C thermal cure denatured the MABSA and virtually eliminated rehydration, resulting in a dMABSA-TA bioplastic.

2. EXPERIMENTAL SECTION

2.1 Methacrylation of BSA. A previously published method for methacrylation of BSA was used.[30] In short, BSA (20 g, 0.3 mmol) and $NaHCO_3$ / Na_2CO_3 buffer (200 mL, 0.25 M, pH 9.0) were added to a 1000 mL round-bottom flask equipped with a magnetic stir bar. The mixture was stirred at 2–8 °C until the BSA dissolved completely. Then, methacrylic anhydride (4 mL, 27 mmol) was added dropwise to the BSA solution over 10 min. The reaction mixture was stirred at 2–8 °C for 2 h. The crude product was diluted two-fold with deionized (DI) water and then dialyzed against DI water for 48 h at 2–8 °C. After dialysis, the product was lyophilized with yields typically > 91.5%. The percent functionalization of the available lysines of BSA with methacryloyl functionalities was determined to be 85-95% using a 2,4,6-trinitrobenzene sulfonate (TNBS) assay.[30]

2.2 Preparation of MABSA-based resin for vat photopolymerization. Three resin formulations were used in this study, each with 30 wt% MABSA and the minimum amount of co-monomer that afforded a printable resin: 5 wt% for poly(ethylene glycol) diacrylate (PEGDA), 3 wt% for acrylamide (AAm), and 2 wt% for 2-hydroxyethyl acrylate (HEA). All stated weight percentages were calculated from the total (final) composition of the resin, including mass of DI water as the solvent. As a representative example, we describe here the preparation 6 g of the resin with 30 wt% MABSA and 5 wt% PEGDA. First, 0.3 g of PEGDA was dissolved in 3.66 mL of DI water; then, 1.8 g of MABSA was slowly added to this solution with gentle mixing until dissolved. Finally, 0.075 wt% $Ru(bpy)_3Cl_2$ was dissolved in 120 μL of DI water, and 0.24 wt% SPS was dissolved in 120 μL of DI water; these solutions were sequentially added to the resin formulation with gentle mixing. The final resin formulation was covered with aluminum foil and stored at 4

°C until use. To prepare the other formulations, similar procedures were followed, changing only the co-monomer and DI water quantity. For fabrication of the bioplastic screw, 0.075 wt% New Coccine was included in the resin formulation. The screw thread geometry was difficult to resolve without inclusion of a photoabsorber. Use of New Coccine as a photoabsorber with this photoinitiator system has been previously reported.[19,50]

2.3 SLA 3D printing of MABSA-based hydrogels. A Formlabs Form 2 printer with a modified build platform and resin tray was used to fabricate the hydrogel constructs.[30] Hydrogel constructs were printed in the Form 2's Open Mode, with a layer height of 100 μm. Upon completion of the print, samples were removed from the build platform, rinsed with DI water to remove uncured resin, and post-cured in a custom photocuring chamber (Quans, 400 nm, 1 mW/cm^2) for 90 min. Some samples were further treated with TA, thermally cured at 120 °C, or treated with both TA and thermally cured.

RESULTS AND DISCUSSION

3.1 Formulation and printability of MABSA-based resins. The MABSA-based resin formulations for SLA 3D printing which we have reported previously[30] afforded printed constructs that only partially degraded in the presence of protease and became mechanically weaker upon swelling in water. We hypothesized that the presence of PEGDA as a non-degradable reactive co-monomer (10 wt% of the resin, 25 wt% of the solids) in these formulations limited the ability of protease to digest the protein network, as the construct only degraded 22% in a concentrated solution of proteinase K (Table S1). We hypothesized that the presence of the nondegradable PEGDA network limited the access of the enzyme to the protein matrix. In this work, we demonstrated fully degradable structures by replacing PEGDA with low molecular weight, monofunctional co-monomers. The use of such co-monomers afforded printable inks at lower co-

monomer concentrations in which enzymatically degradable MABSA served as junctions in the cross-linked network. Finally, the addition of TA as an additive to the printed constructs gave hydrogels and bioplastics that could retain their toughness even in the presence of water.

We investigated three co-monomers as additives in MABSA-based resin formulations: acrylamide (AAm), hydroxyethylacrylate (HEA), and PEGDA. All of the resin formulations investigated comprised 30 wt% MABSA, with 0.075 wt% $Ru(bpy)_3Cl_2$ and 0.24 wt% sodium persulfate (SPS) as the photoinitiating system. The minimum quantity of co-monomer additive required to produce a printable resin was determined by printing cylinders using a Form 2 printer with 1–10 wt% of co-monomer. We observed that resin formulations with < 3 wt% AAm, < 2 wt% HEA, or < 5 wt% PEGDA exhibited insufficient photocuring rates, which resulted in delamination between layers and failed prints (Figure S1). At equal or greater values than these respective concentrations of co-monomer, we consistently obtained successful prints. These minimum concentrations of co-monomer (3 wt% AAm, 2 wt% HEA, and 5 wt% PEGDA) were used in all subsequent experiments.

3.2 MABSA-TA interactions. For each of the formulations, we investigated post-print processing of the printed constructs with TA to increase toughness of the materials. The as-printed constructs were immersed in a solution of 300 mg/mL TA for 72 h to infuse TA into the polymer matrix to afford MABSA-TA composite hydrogels. We hypothesized that the incorporation of noncovalent interactions (primarily hydrogen bonding) between MABSA and TA would improve the toughness of these materials by providing a mechanism for energy dissipation. FTIR spectra of the MABSA-TA network hydrogel showed that the peak representing TA carbonyl groups shifted from 1700 to 1721 cm^{-1}, confirming the formation of hydrogen bonds between TA and the printed MABSA structures (Figure S4). Gravimetric analysis of the samples showed that the

masses of the dehydrated TA composites were higher than those before TA infusion and contained up to 25 wt% TA relative to the total dry mass (Table S3).

To investigate how TA influences the swelling behavior of the printed constructs, different treatments including TA treatment, 120 °C thermal cure, and the combination of the two treatments (TA and 120 °C thermal cure) were performed. After the TA treatment, the swelling ratio of the MABSA-AAm, MABSA-HEA, and MABSA-PEGDA hydrogels reduced by more than 50% for each formulation (Figure 2). We have shown previously that thermal curing of photocured MABSA results in loss of α-helix structure with concomitant formation of intermolecular β-sheets.[51] Separately, the thermal cure and TA treatment each decreased the swelling ratio of the printed constructs in water by roughly the same amount. Interestingly, a combination of TA treatment followed by 120 °C thermal cure greatly reduced the swelling ratio to below 0.11 for all formulations (Figure 2). (add crosslink data response to reviewer)

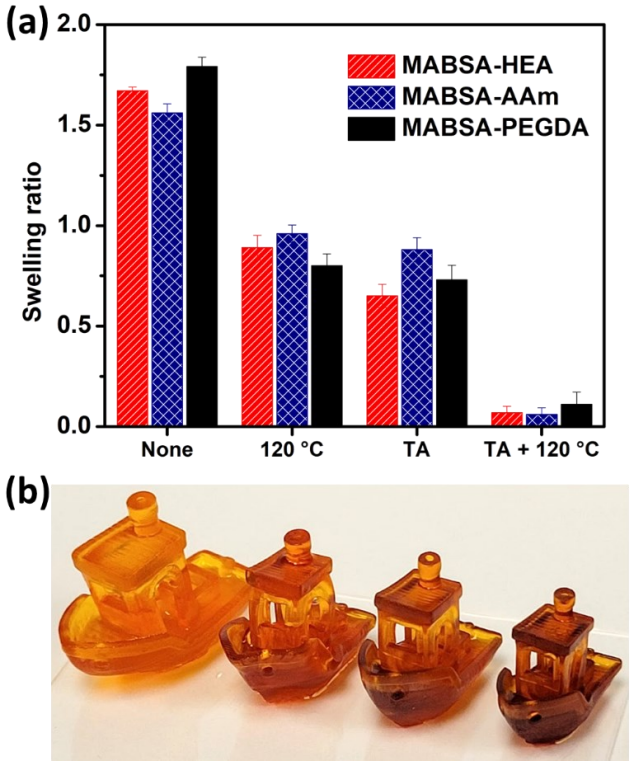

Figure 2. (a) Swelling ratios of 3D printed MABSA-based formulations after each post-print treatment, including: no treatment, 120 °C thermal cure, TA treatment, and TA treatment and 120 °C thermal cure; (b) Image of 3D printed MABSA-HEA constructs at equilibrium swelling in DI water after each post-print treatment: none, 120 °C thermal cure, TA treatment, and TA treatment and thermal cure (from left to right).

3.3 Effect of post-print treatments on mechanical properties. The uniaxial tensile mechanical properties of the cured materials (ultimate strength, toughness, and elastic modulus) were quantified using a load frame (Figure 3a-f). Among the non-treated hydrogels, MABSA-AAm had the highest Young's modulus (2.02 MPa), which was ~ 3 times greater than those of MABSA-HEA (0.64 MPa) and MABSA-PEGDA (0.68 MPa) (Figure 3d). Similarly, MABSA-AAm demonstrated the highest ultimate strength and toughness (Figure 3e,f). These results are likely due to the additional hydrogen bonding interactions between the acrylamide groups and MABSA. The TA treatment afforded higher ultimate strength and toughness for all formulations. When compared to the non-treated samples, the ultimate strength increased 27-fold for MABSA-HEA-TA, 3.4-fold for MABSA-AAm-TA, and 15-fold for MABSA-PEGDA-TA. These improvements are attributed to energy dissipation afforded by the disruption of hydrogen bonding and other noncovalent interactions under tensile strain.[42,52–54] The increased hydrogen bonding interactions that are introduced with the presence of TA in the matrix decreased the water uptake by the materials and also improved the mechanical properties of the hydrogels. Finally, the samples that were thermally cured at 120 °C after the TA treatment exhibited the greatest improvements in mechanical properties. The ultimate strength increased to 7.1 MPa for dMABSA-HEA-TA, 3.2 MPa for dMABSA-AAm-TA, and 3.8 MPa for dMABSA-PEGDA-TA. These increases in

mechanical strength were also accompanied by significant reductions in water uptake. Thus, post-print TA treatment followed by thermal curing transforms the as-printed hydrogels into bioplastics (which show minimal rehydration in water, Figure 2b).

To demonstrate the high mechanical strength of these 3D printed bioplastics, a mechanically functional screw was fabricated. The MABSA-PEGDA resin was formulated with 0.075 wt% New Coccine (a red food dye). In particular, for 3D printing a screw, we found it beneficial to include the dye to enhance the resolution of the screw threads.[19] Following TA treatment and thermal curing, the screw was successfully driven into a piece of balsa wood and then removed without any visible structural damage to the screw (Figure 3h).

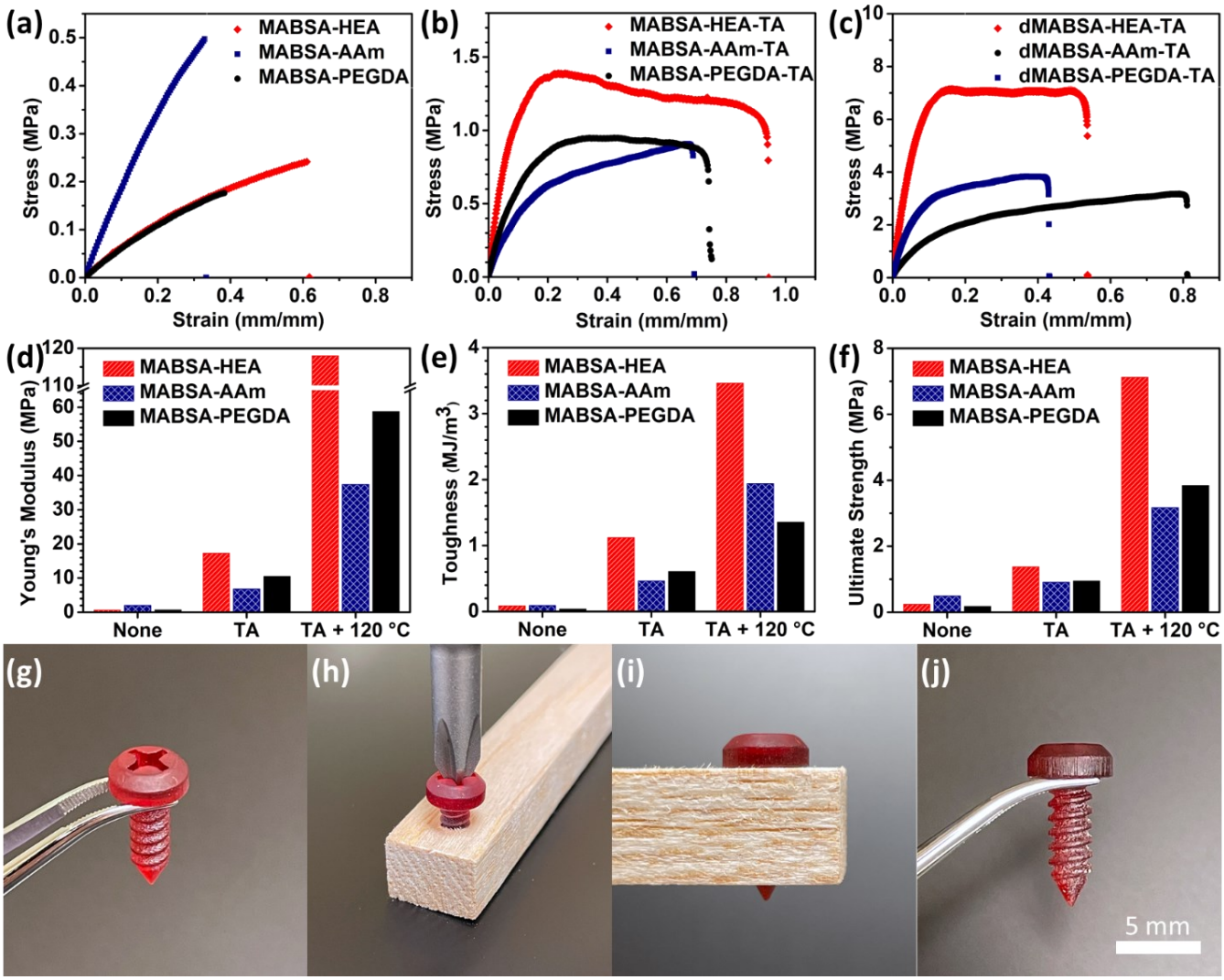

Figure 3. Tensile stress-strain curves of all formulations at equilibrium swelling (a) with no post-print treatment, (b) after TA treatment, (c) after TA treatment and 120 °C thermal cure. (d) Young's modulus, (e) toughness, and (f) Ultimate strength of each formulation with no post-print treatment, 120 °C thermal cure, TA treatment, and both TA treatment and 120 °C thermal cure. (g) 3D printed bioplastic screw after TA treatment and 120 °C thermal cure. (h) Bioplastic screw being driven into wood. (i) Side view of bioplastic screw in wood, (j) Bioplastic screw after removal from wood, lacking visible damage.

3.4 Biodegradation. All of the resin compositions afforded biodegradable materials with degradation rates that depended upon the material composition and post-print processing conditions. The biodegradability of these materials was investigated over the course of 30 d in a pepsin solution (pH 1.5–2.0) at 37 °C. Without any post-print treatment, the samples degraded 46.0%, 61.2%, and 59.9% for MABSA-HEA, MABSA-AAm, and MABSA-PEGDA, respectively (Figure 4). Regardless of co-monomer used, the samples with TA treatment exhibited the greatest mass loss, 75.3% for MABSA-HEA-TA, 67.5% for MABSA-AAm-TA, and 85.0% for MABSA-PEGDA-TA. This increase in degradation could be the result of TA disrupting protein interactions and providing the enzyme with greater access to cleavage sites.[55] Additionally, polyphenols have been shown to enhance the activity of pepsin.[56] Samples that were treated with TA and cured at 120 °C exhibited the lowest degradation rates. This is likely due to the low water uptake of these materials, which could limit pepsin transport into the material, thus limiting degradation.

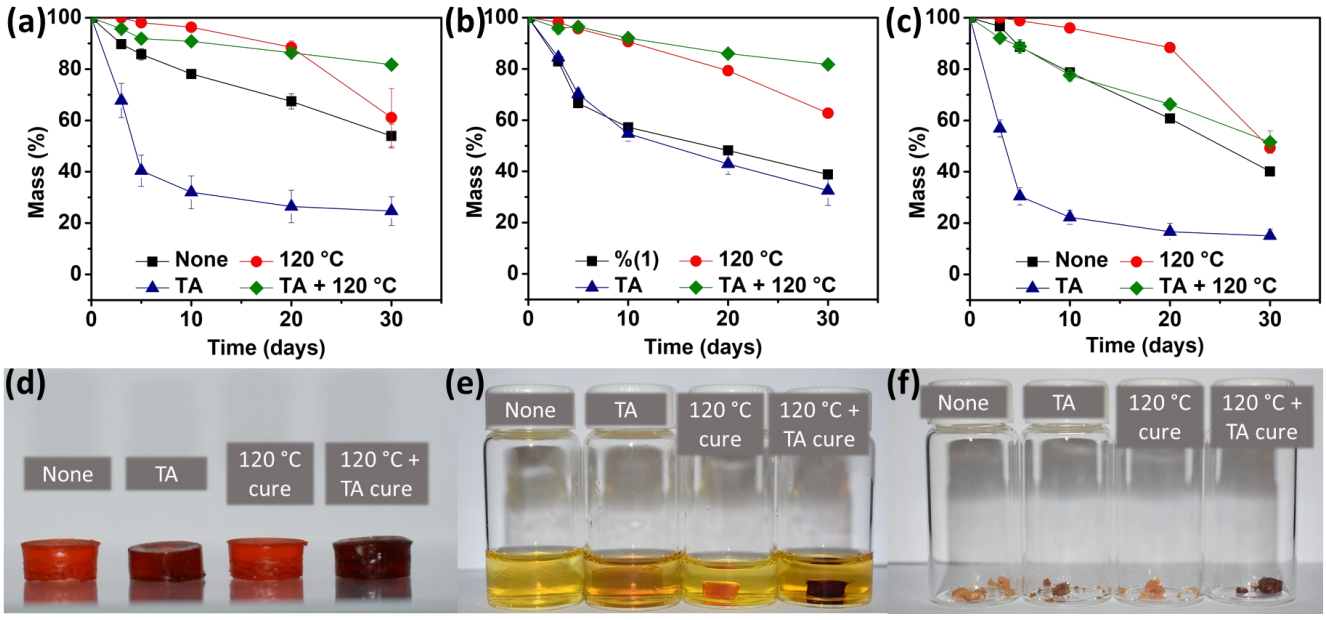

Figure 4. Degradation of printed constructs over 30 d in pepsin solution (a) MABSA-HEA, (b) MABSA-AAm, (c) MABSA-PEGDA. Images of MABSA-HEA, MABSA-HEA-TA, dMABSA-

HEA, and dMABSA-HEA-TA at (d) day 0 prior to incubation in pepsin solution, (e) after 5 d incubation in pepsin solution, (f) after 30 d incubation in pepsin solution.

3.5 Suturing. To further demonstrate the excellent mechanical functionality of these MABSA-based hydrogels, we qualitatively investigated the response of the materials to suturing (Figure 5). The MABSA-based hydrogels without post-print treatments were brittle and exhibited visible crack propagation throughout the material upon insertion of the suture needle, as shown in Figure 5a. Interestingly, after TA treatment, a 3 mm thick sample exhibited markedly reduced crack propagation (Figure 5b) and could support 500 g loaded on a single loop of suture material (Figure 5c). To demonstrate suturing to tissue, a hydrogel patch (~ 8 mm × 8 mm) was 3D printed and treated with TA. A square of matching size was cut from a section of bovine small intestine. After equilibration in water, the hydrogel patch was sutured in place. The sutures held firmly even after 24 h of water immersion (Figure 5f and 5g).

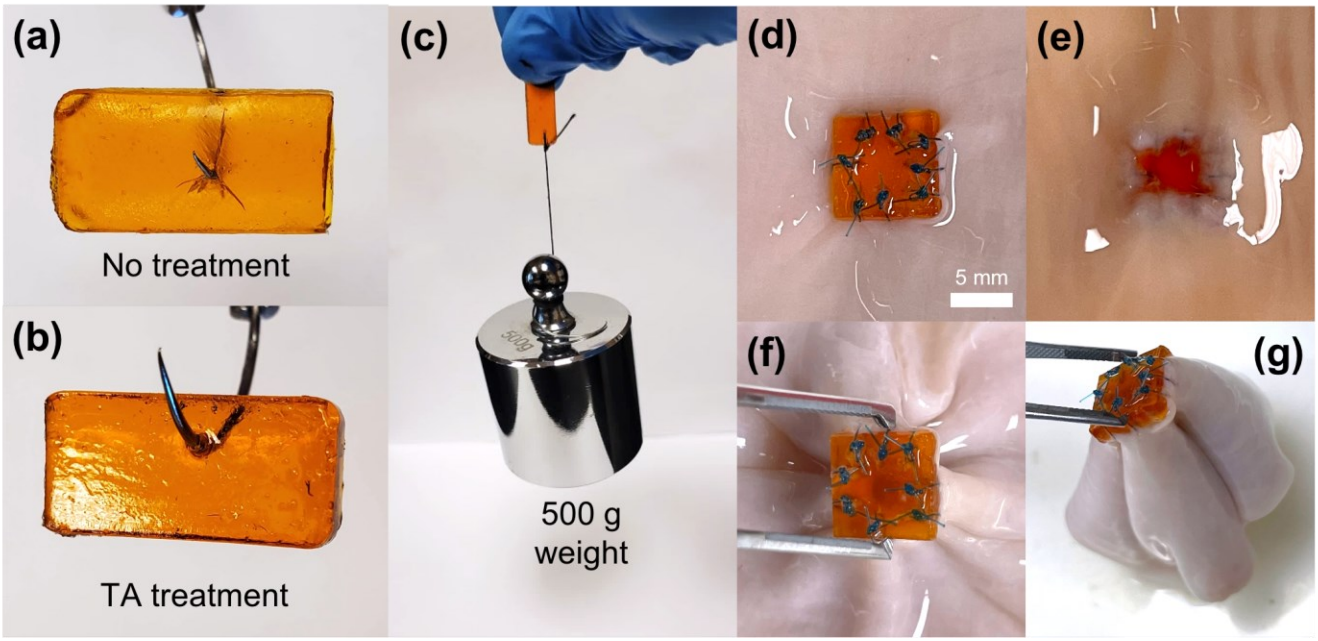

Figure 5. Images showing the suturability of MABSA-HEA hydrogels. Piercing a 3D printed hydrogel strip with a suture needle (a) with no post-print treatment (MABSA-HEA hydrogel) and (b) after TA treatment (MABSA-HEA-TA hydrogel). (c) MABSA-HEA-TA hydrogel strip supporting a 500 g weight via a single loop of suture material. (d, e) MABSA-HEA-TA hydrogel patch sutured to bovine small intestine, with front and back views shown respectively. (f, g) MABSA-HEA-TA patch sutured to bovine small intestine after immersion in water for 24 h.

4. CONCLUSION

In summary, we developed an additive manufacturing process using MABSA and TA to fabricate tough, protein-based hydrogels and bioplastics. The 3D printed constructs exhibited excellent mechanical properties (elastic modulus, strength, and toughness) and can biodegrade in the presence of a pepsin protease. A mechanically functional screw was 3D printed to showcase the utility of this process to afford bioplastic constructs. We also developed tough hydrogels that could withstand a suturing process and demonstrated the robustness of the material even after submersion in water. The broad range of mechanical properties achievable with this platform affords opportunities for 3D printable and degradable bioplastics and hydrogels. In the future, we envision these materials will enable customized 3D printed stents, patches, and drug delivery devices that can degrade *in situ*.

AUTHOR INFORMATION

Corresponding Author

* Alshakim Nelson. Department of Chemistry, University of Washington, Seattle, Washington 98195, USA. Email: alshakim@uw.edu

Present Addresses

† Molecular Engineering and Sciences Institute, University of Washington

┠ Department of Surgery, University of Washington, Seattle, WA 98195, USA

Author Contributions

The manuscript was written through contributions of all authors. All authors have given approval to the final version of the manuscript.

Supporting Information

Materials and detailed experimental procedures are provided; supporting images, tabulated data (rheology, TA concentration, compression and tensile properties, and change in dimensions following each post-print treatment), degradation data, and ATR-FTIR spectra.

ACKNOWLEDGMENT

This work was supported by the Office of the Assistant Secretary of Defense for Health Affairs through the CDMRP under Award No. (W81XWH-21-1-0167). We also thank the National Science Foundation (1752972) for partial support of this project.

REFERENCES

(1) Schneiderman, D. K.; Hillmyer, M. A. 50th Anniversary Perspective: There Is a Great

Future in Sustainable Polymers. *Macromolecules* **2017**, *50* (10), 3733–3749.

(2) Geyer, R.; Jambeck, J. R.; Law, K. L. Production, Use, and Fate of All Plastics Ever Made. *Sci. Adv.* **2017**, *3* (7), 25–29.

(3) O'dea, R. M.; Willie, J. A.; Epps, T. H. 100th Anniversary of Macromolecular Science Viewpoint: Polymers from Lignocellulosic Biomass. Current Challenges and Future Opportunities. *ACS Macro Lett.* **2020**, *9* (4), 476–493.

(4) Sanchez-Rexach, E.; Johnston, T. G.; Jehanno, C.; Sardon, H.; Nelson, A. Sustainable Materials and Chemical Processes for Additive Manufacturing. *Chem. Mater.* **2020**, *32* (17), 7105–7119.

(5) Pirsa, S.; Sharifi, K. A. A Review of the Applications of Bioproteins in the Preparation of Biodegradable Films and Polymers. *J. Chem. Lett.* **2020**, *1*, 47–58.

(6) Mohamed, S. A. A.; El-Sakhawy, M.; El-Sakhawy, M. A. M. Polysaccharides, Protein and Lipid -Based Natural Edible Films in Food Packaging: A Review. *Carbohydr. Polym.* **2020**, *238* (March), 116178.

(7) Giaveri, S.; Schmitt, A. M.; Roset Julià, L.; Scamarcio, V.; Murello, A.; Cheng, S.; Menin, L.; Ortiz, D.; Patiny, L.; Bolisetty, S.; Mezzenga, R.; Maerkl, S. J.; Stellacci, F. Nature-Inspired Circular-Economy Recycling for Proteins: Proof of Concept. *Adv. Mater.* **2021**, *33* (44):e2104581.

(8) Hernandez-Izquierdo, V. M.; Krochta, J. M. Thermoplastic Processing of Proteins for Film Formation - A Review. *J. Food Sci.* **2008**, *73* (2), R30–R39.

(9) Kapoor, S.; Kundu, S. C. Silk Protein-Based Hydrogels: Promising Advanced Materials for

Biomedical Applications. *Acta Biomater.* **2016**, *31*, 17–32.

(10) Bagheri, A.; Jin, J. Photopolymerization in 3D Printing. *ACS Appl. Polym. Mater.* **2019**, *1* (4), 593–611.

(11) Appuhamillage, G. A.; Chartrain, N.; Meenakshisundaram, V.; Feller, K. D.; Williams, C. B.; Long, T. E. 110th Anniversary: Vat Photopolymerization-Based Additive Manufacturing: Current Trends and Future Directions in Materials Design. *Ind. Eng. Chem. Res.* **2019**, *58* (33), 15109–15118.

(12) Tumbleston, J. R.; Shirvanyants, D.; Ermoshkin, N.; Janusziewicz, R.; Johnson, A. R.; Kelly, D.; Chen, K.; Pinschmidt, R.; Rolland, J. P.; Ermoshkin, A.; Samulski, E. T.; DeSimone, J. M. Continuous Liquid Interface Production of 3D Objects. *Science (80-.).* **2015**, *347* (6228), 1349–1352.

(13) Walker, D. A.; Hedrick, J. L.; Mirkin, C. A. Rapid, Large-Volume, Thermally Controlled 3D Printing Using a Mobile Liquid Interface. *Science (80-.).* **2019**, *366*, 360–364.

(14) Zuev, D. M.; Nguyen, A. K.; Putlyaev, V. I.; Narayan, R. J. 3D Printing and Bioprinting Using Multiphoton Lithography. *Bioprinting* **2020**, *20*, e00090.

(15) Poldervaart, M. T.; Goversen, B.; De Ruijter, M.; Abbadessa, A.; Melchels, F. P. W.; Öner, F. C.; Dhert, W. J. A.; Vermonden, T.; Alblas, J. 3D Bioprinting of Methacrylated Hyaluronic Acid (MeHA) Hydrogel with Intrinsic Osteogenicity. *PLoS One* **2017**, *12* (6), 1–15.

(16) Lim, K. S.; Schon, B. S.; Mekhileri, N. V.; Brown, G. C. J.; Chia, C. M.; Prabakar, S.; Hooper, G. J.; Woodfield, T. B. F. New Visible-Light Photoinitiating System for Improved

Print Fidelity in Gelatin-Based Bioinks. *ACS Biomater. Sci. Eng.* **2016**, *2* (10), 1752–1762.

(17) Ding, R.; Du, Y.; Goncalves, R. B.; Francis, L. F.; Reineke, T. M. Sustainable near UV-Curable Acrylates Based on Natural Phenolics for Stereolithography 3D Printing. *Polym. Chem.* **2019**, *10* (9), 1067–1077.

(18) Kim, S. H.; Yeon, Y. K.; Lee, J. M.; Chao, J. R.; Lee, Y. J.; Seo, Y. B.; Sultan, M. T.; Lee, O. J.; Lee, J. S.; Yoon, S. Il; Hong, I. S.; Khang, G.; Lee, S. J.; Yoo, J. J.; Park, C. H. Precisely Printable and Biocompatible Silk Fibroin Bioink for Digital Light Processing 3D Printing. *Nat. Commun.* **2018**, *9*, 1620.

(19) Castilho, M. D.; Malda, J.; Levato, R.; Alcala-Orozco, C. R.; Melchels, F. P. W.; Gawlitta, D.; Hooper, G. J.; Woodfield, T. B. F.; Costa, P. F.; Lim, K. S.; van Dorenmalen, K. M. A. Bio-Resin for High Resolution Lithography-Based Biofabrication of Complex Cell-Laden Constructs. *Biofabrication* **2018**, *10* (3), 034101.

(20) Schüller-Ravoo, S.; Teixeira, S. M.; Feijen, J.; Grijpma, D. W.; Poot, A. A. Flexible and Elastic Scaffolds for Cartilage Tissue Engineering Prepared by Stereolithography Using Poly(Trimethylene Carbonate)-Based Resins. *Macromol. Biosci.* **2013**, *13* (12), 1711–1719.

(21) Elomaa, L.; Teixeira, S.; Hakala, R.; Korhonen, H.; Grijpma, D. W.; Seppälä, J. V. Preparation of Poly(ε-Caprolactone)-Based Tissue Engineering Scaffolds by Stereolithography. *Acta Biomater.* **2011**, *7* (11), 3850–3856.

(22) Hinczewski, C.; Corbel, S.; Chartier, T. Ceramic Suspensions Suitable for Stereolithography. *J. Eur. Ceram. Soc.* **1998**, *18* (6), 583–590.

(23) Sutton, J. T.; Rajan, K.; Harper, D. P.; Chmely, S. C. Lignin-Containing Photoactive Resins

for 3D Printing by Stereolithography. *ACS Appl. Mater. Interfaces* **2018**, *10* (42), 36456–36463.

(24) Luo, Y.; Le Fer, G.; Dean, D.; Becker, M. L. 3D Printing of Poly(Propylene Fumarate) Oligomers: Evaluation of Resin Viscosity, Printing Characteristics and Mechanical Properties. *Biomacromolecules* **2019**, *20* (4), 1699–1708.

(25) Hiemenz, P. C.; Lodge, T. *Polymer Chemistry*, 2nd ed.; CRC Press, 2007.

(26) Seiler, M. Hyperbranched Polymers: Phase Behavior and New Applications in the Field of Chemical Engineering. *Fluid Phase Equilib.* **2006**, *241*, 155–174.

(27) Voit, B. I.; Lederer, A. Hyperbranched and Highly Branched Polymer Architectures-Synthetic Strategies and Major Characterization Aspects. *Chem. Rev.* **2009**, *109* (11), 5924–5973.

(28) Le Fer, G.; Luo, Y.; Becker, M. L. Poly(Propylene Fumarate) Stars, Using Architecture to Reduce the Viscosity of 3D Printable Resins. *Polym. Chem.* **2019**, *10* (34), 4655–4664.

(29) Ryan J. Mondschein, Akanksha Kanitkar, Christopher B. Williamsb,Scott S. Verbridge, T. E. L. Polymer Structure-Property Requirements for Stereolithographic 3Dprinting of Soft Tissue Engineering Scaffolds. *Biomaterials* **2017**, *140*, 170–188.

(30) Smith, P. T.; Narupai, B.; Tsui, J. H.; Millik, S. C.; Shafranek, R. T.; Kim, D. H.; Nelson, A. Additive Manufacturing of Bovine Serum Albumin-Based Hydrogels and Bioplastics. *Biomacromolecules* **2020**, *21* (2), 484–492.

(31) Yin, J.; Yan, M.; Wang, Y.; Fu, J.; Suo, H. 3D Bioprinting of Low-Concentration Cell-Laden Gelatin Methacrylate (GelMA) Bioinks with a Two-Step Cross-Linking Strategy.

ACS Appl. Mater. Interfaces **2018**, *10* (8), 6849–6857.

(32) Xing, Q.; Yates, K.; Vogt, C.; Qian, Z.; Frost, M. C.; Zhao, F. Increasing Mechanical Strength of Gelatin Hydrogels by Divalent Metal Ion Removal. *Sci. Rep.* **2014**, *4*, 1–10.

(33) Nonoyama, T.; Gong, J. P. Tough Double Network Hydrogel and Its Biomedical Applications. *Annu. Rev. Chem. Biomol. Eng.* **2021**, *12*, 393–410.

(34) Johari, N.; Moroni, L.; Samadikuchaksaraei, A. Tuning the Conformation and Mechanical Properties of Silk Fibroin Hydrogels. *Eur. Polym. J.* **2020**, *134* (February), 109842.

(35) Zhao, X.; Chen, X.; Yuk, H.; Lin, S.; Liu, X.; Parada, G. Soft Materials by Design: Unconventional Polymer Networks Give Extreme Properties. *Chem. Rev.* **2021**, *121* (8), 4309–4372.

(36) Peak, C. W.; Wilker, J. J.; Schmidt, G. A Review on Tough and Sticky Hydrogels. *Colloid Polym. Sci.* **2013**, *291* (9), 2031–2047.

(37) Zhou, X.; Li, C.; Zhu, L.; Zhou, X. Engineering Hydrogels by Soaking: From Mechanical Strengthening to Environmental Adaptation. *Chem. Commun.* **2020**, *56* (89), 13731–13747.

(38) Zhang, C.; Liu, Z.; Shi, Z.; Li, T.; Xu, H.; Ma, X.; Yin, J.; Tian, M. Inspired by Elastomers: Fabrication of Hydrogels with Tunable Properties and Re-Shaping Ability: Via Photo-Crosslinking at a Macromolecular Level. *Polym. Chem.* **2017**, *8* (11), 1824–1832.

(39) Sun, W.; Xue, B.; Fan, Q.; Tao, R.; Wang, C.; Wang, X.; Li, Y.; Qin, M.; Wang, W.; Chen, B.; Cao, Y. Molecular Engineering of Metal Coordination Interactions for Strong, Tough, and Fast-Recovery Hydrogels. *Sci. Adv.* **2020**, *6* (16):eaaz9531.

(40) Zheng, S. Y.; Ding, H.; Qian, J.; Yin, J.; Wu, Z. L.; Song, Y.; Zheng, Q. Metal-Coordination Complexes Mediated Physical Hydrogels with High Toughness, Stick-Slip Tearing Behavior, and Good Processability. *Macromolecules* **2016**, *49* (24), 9637–9646.

(41) Nakahata, M.; Takashima, Y.; Harada, A. Highly Flexible, Tough, and Self-Healing Supramolecular Polymeric Materials Using Host-Guest Interaction. *Macromol. Rapid Commun.* **2016**, *37* (1), 86–92.

(42) Gonzalez, M. A.; Simon, J. R.; Ghoorchian, A.; Scholl, Z.; Lin, S.; Rubinstein, M.; Marszalek, P.; Chilkoti, A.; López, G. P.; Zhao, X. Strong, Tough, Stretchable, and Self-Adhesive Hydrogels from Intrinsically Unstructured Proteins. *Adv. Mater.* **2017**, *29* (10), 1–8.

(43) Zhao, X. Multi-Scale Multi-Mechanism Design of Tough Hydrogels: Building Dissipation into Stretchy Networks. *Soft Matter* **2014**, *10* (5), 672–687.

(44) Quideau, S.; Deffieux, D.; Douat-Casassus, C.; Pouységu, L. Plant Polyphenols: Chemical Properties, Biological Activities, and Synthesis. *Angew. Chemie - Int. Ed.* **2011**, *50* (3), 586–621.

(45) Chen, Y.; Hagerman, A. E. Characterization of Soluble Non-Covalent Complexes between Bovine Serum Albumin and β-1,2,3,4,6-Penta-O-Galloyl-D-Glucopyranose by MALDI-TOF MS. *J. Agric. Food Chem.* **2004**, *52* (12), 4008–4011.

(46) Labieniec, M.; Gabryelak, T. Interactions of Tannic Acid and Its Derivatives (Ellagic and Gallic Acid) with Calf Thymus DNA and Bovine Serum Albumin Using Spectroscopic Method. *J. Photochem. Photobiol. B Biol.* **2006**, *82* (1), 72–78.

(47) Smith, P. T. Additive Manufacturing of Bovine Serum Albumin-Based and Pluronic F127 Hydrogels and Bioplastics. Ph.D. Dissertation, University of Washington, Seattle, WA, 2021.

(48) Lu, R.; Li, W. W.; Katzir, A.; Raichlin, Y.; Yu, H. Q.; Mizaikoff, B. Probing the Secondary Structure of Bovine Serum Albumin during Heat-Induced Denaturation Using Mid-Infrared Fiberoptic Sensors. *Analyst* **2015**, *140* (3), 765–770.

(49) Shanmugam, G.; Polavarapu, P. L. Vibrational Circular Dichroism Spectra of Protein Films: Thermal Denaturation of Bovine Serum Albumin. *Biophys. Chem.* **2004**, *111* (1), 73–77.

(50) Field, J.; Haycock, J. W.; Boissonade, F. M.; Claeyssens, F. A Tuneable, Photocurable, Poly(Caprolactone)-Based Resin for Tissue Engineering-Synthesis, Characterisation and Use in Stereolithography. *Molecules* **2021**, *26* (5), 1199.

(51) Sanchez-Rexach, E.; Smith, P. T.; Gomez-Lopez, A.; Fernandez, M.; Cortajarena, A. L.; Sardon, H.; Nelson, A. 3D-Printed Bioplastics with Shape-Memory Behavior Based on Native Bovine Serum Albumin. *ACS Appl. Mater. Interfaces* **2021**, *13* (16), 19193–19199.

(52) Fang, J.; Mehlich, A.; Koga, N.; Huang, J.; Koga, R.; Gao, X.; Hu, C.; Jin, C.; Rief, M.; Kast, J.; Baker, D.; Li, H. Forced Protein Unfolding Leads to Highly Elastic and Tough Protein Hydrogels. *Nat. Commun.* **2013**, *4,* 2974.

(53) Zhao, L.; Zhang, X.; Luo, Q.; Hou, C.; Xu, J.; Liu, J. Engineering Nonmechanical Protein-Based Hydrogels with Highly Mechanical Properties: Comparison with Natural Muscles. *Biomacromolecules* **2020**, *21* (10), 4212–4219.

(54) Da Silva, M. A.; Lenton, S.; Hughes, M.; Brockwell, D. J.; Dougan, L. Assessing the

Potential of Folded Globular Polyproteins As Hydrogel Building Blocks. *Biomacromolecules* **2017**, *18* (2), 636–646.

(55) Osawa, R.; Walsh, T. Effects of Acidic and Alkaline Treatments on Tannic Acid and Its Binding Property to Protein. *J. Agric. Food Chem* **1993**, *41*, 704–707.

(56) Tagliazucchi, D.; Verzelloni, E.; Conte, A. Effect of Some Phenolic Compounds and Beverages on Pepsin Activity during Simulated Gastric Digestion. *J. Agric. Food Chem.* **2005**, *53* (22), 8706–8713.

TOC